Thermal Decomposition of Platinum(IV)−Silicon, −Germanium, and −Tin Complexes

Christopher J. Levy and Richard J. Puddephatt*

Department of Chemistry, The University of Western Ontario, London, Ontario, Canada N6A 5B7

Received March 12, 1997[⊗]

The thermal decomposition of a number of complexes of the type $[PtMe_2(Me_3E)X(diimine)]$ (E = Si, Ge, Sn; X = Cl, Br, I) has been studied. The thermal stability of complexes, as determined by thermogravimetric analysis (TGA), varies depending on the diimine ligand in the order 2,2′-bipyridyl (bpy) > 4,4′-di-*tert*-butyl-2,2′-bipyridyl (bpy-^{t}bu$_2$) > *N*-(2-(dimethylamino)ethyl)pyridine-2-aldimine (paen-me$_2$) > (2-imino-*n*-propyl)pyridine (py-*n*-pr). Stability also varies according to the trends E = Sn ≈ Ge > Si and X = I > Br > Cl. The products of thermal decomposition have also been determined by ^{1}H NMR and three distinct modes of decomposition are evident: reductive elimination of Me_3EX, reductive elimination of Me_4E, and α-elimination of Me_2E. The competition between reductive elimination of Me_3EX and Me_4E depends primarily on the halide, X, with the ratio Me_3EX:Me_4E highest for X = Cl and lowest for X = I. The competition between reductive elimination and α-elimination depends primarily on E, with the tendency to α-elimination of Me_2E increasing as E = Si < Ge < Sn. Differential scanning calorimetry (DSC) has been used to estimate *D*(Pt−Si) for the complex $[PtIMe_2(Me_3Si)(bpy)]$ as 233 ± 14 kJ mol^{-1}.

Introduction

Although oxidative addition of alkyl halides has been studied in depth, there are surprisingly few examples of selective reductive elimination of alkyl halides from alkylhalometal complexes.[1] In 1959, Chatt and Shaw reported that reductive elimination from halomethylplatinum(IV) complexes generally produces mixtures of methyl halides and ethane, while Ruddick and Shaw found that platinum(IV) complexes containing at least two halogens and one or two methyl groups yield methyl halide on thermolysis (185−210 °C).[2] In dihalodimethylplatinum(IV) complexes, the selectivity for reductive elimination of MeX or C_2H_6 depends on the nature of the halogen and the geometry of the complex. Recently, a report of competitive C−C and C−I reductive elimination from $[PtIMe_3(dppe)]$ has been published.[3] When the platinum(IV) complex is heated in acetone-d_6, initial reductive elimination of (predominantly) methyl iodide was observed by NMR spectroscopy, but with extended heating, all material was converted to ethane and [PtIMe(dppe)]. Since the oxidative addition of Me_3EX to $[PtMe_2(diimine)]$ (E = Si, Ge, Sn; X = Cl, Br, I) is rapid and reversible in solution, a study of the solid-state thermolysis of the products $[PtMe_2(Me_3E)X(diimine)]$ was carried out.[4] Three different decomposition modes were identified, as reported below.

Bond dissociation energies of organometallic complexes are usually difficult to obtain, and there are few experimental or theoretical estimates of metal−silicon bond dissociation energies.[5] One method which has been used extensively to find heats of reactions in inorganic and organometallic chemistry is differential scanning calorimetry (DSC). We have used this technique to study the decomposition of $[PtIMe_2(Me_3Si)(bpy)]$ and have obtained a value for *D*(Pt−Si) in this complex. A preliminary report on this part of the research has been published,[4] and the synthesis of the platinum(IV) complexes has been described.[6]

Results

TGA of Platinum(IV) Complexes. The TGA curves obtained for platinum(IV) complexes are similar in appearance to that shown in Figure 1 (20−800 °C) for $[PtClMe_2(Me_3Sn)(bpy\text{-}^tbu_2)]\cdot Me_3SnCl$, a weak complex of $[PtClMe_2(Me_3Sn)(bpy\text{-}^tbu_2)]\cdot$ with Me_3SnCl. This complex is thermally stable to 120 °C, above which it loses substantial mass in a fairly narrow temperature range (120−160 °C). This initial mass loss (42.7%) could be due to loss of two molecules of Me_3SnCl (44.7%) or one molecule each of Me_3SnCl and Me_4Sn (42.4%). In either case, it is interesting that reductive elimination from the platinum(IV) complex appears to occur nearly simultaneously with loss of the weakly bound Me_3SnCl molecule. The decomposition product is stable up to 220 °C, and then it loses mass in a second decomposition step (220−290 °C). The mass loss (19.2%) does not correspond to ethane (3.4%), MeCl (5.7%), or bpy-^{t}bu$_2$ (30.1%). Above 290 °C the mass is lost gradually and, at 800 °C, the remaining residue has a mass percent

[⊗] Abstract published in *Advance ACS Abstracts,* August 15, 1997.

(1) Stille, J. K. In *The Chemistry of the Metal-Carbon Bond: The Nature and Cleavage of Metal-Carbon Bonds*; Hartley, F. R., Patai, S., Eds.; Wiley: Toronto, 1985; p 745.

(2) (a) Chatt, J.; Shaw, B. L. *J. Chem. Soc.* **1959**, 705. (b) Ruddick, J. D.; Shaw, B. L. *J. Chem. Soc., A* **1969**, 2969.

(3) (a) Goldberg, K. I.; Yan, J.; Winter, E. L. *J. Am. Chem. Soc.* **1994**, *116*, 1573. (b) Goldberg, K. I.; Yan, J.; Breitung, E. M. *J. Am. Chem. Soc.* **1995**, *117*, 6889.

(4) Levy, C. J.; Puddephatt, R. J. *Organometallics* **1995**, *14*, 5019.

(5) (a) Nolan, S. P.; Porchia, M.; Marks, T. J. *Organometallics* **1991**, *10*, 1450. (b) Jiang, Q.; Pestana, D. C.; Carroll, P. J.; Berry, D. H. *Organometallics* **1994**, *13*, 3679. (c) Ziegler, T.; Tschinke, V.; Versluis, L.; Baerends, E. J.; Ravenek, W. *Polyhedron* **1988**, *7*, 1625. (d) Tilley, T. D. In *The Silicon-Heteroatom Bond*; Patai, S., Rappoport, Z., Eds.; Wiley: New York, 1991; pp 245, 309.

(6) Levy, C. J.; Puddephatt, R. J. *Organometallics* **1996**, *15*, 2108.

S0276-7333(97)00204-5 CCC: $14.00

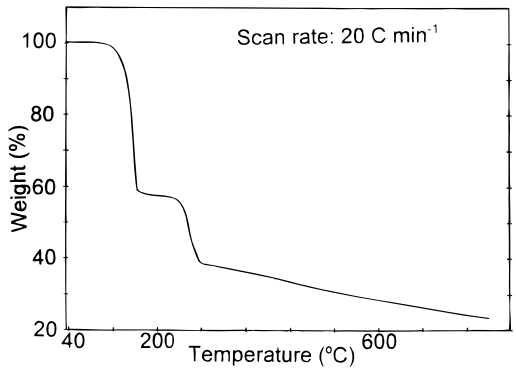

Figure 1. TGA curve of [$PtClMe_2(Me_3Sn)(bpy\text{-}^tbu_2)$].

(23%) close to the platinum content in the original complex (21.9%), indicating almost complete decomposition of the sample. Most platinum(IV) complexes studied in this work undergo an initial decomposition step in a fairly narrow temperature range, similar to that observed for [$PtClMe_2(Me_3Sn)(bpy\text{-}^tbu_2)$]·$Me_3SnCl$. However, subsequent decomposition often occurs in multiple, overlapping steps. Table 1 contains TGA data for the first decomposition step of those platinum(IV) complexes studied. There is a clear trend for increased thermal stability with increased halide size, as can be seen in the TGA curves for the complexes [$PtMe_2X(Me_3Sn)(bpy)$] (X = Cl, Br, I) in Figure 2.

^{1}H NMR Analysis of Decomposition Products. Platinum(IV) complexes were heated under vacuum in NMR tubes, and solutions of the solid and evolved volatiles were examined by ^{1}H NMR spectroscopy. The temperature of pyrolysis was that of the first decomposition step determined by TGA. The product ratios obtained from ^{1}H NMR are presented in Table 2.

The ^{1}H NMR spectra of the solid resulting from the decomposition of [$PtClMe_2(Me_3Sn)(bpy)$] shows several Me−Pt resonances. The most intense of these is due to [$PtMe_2(bpy)$] (δ 0.97, ^2J(PtH) = 86 Hz), indicating major decomposition by the reductive elimination of Me_3SnCl. A minor Me−Pt signal due to [PtClMe(bpy)] (δ 1.05, ^2J(PtH) = 79 Hz),[7] is also present, consistent with Me_4Sn reductive elimination as a minor decomposition pathway. The spectrum shows two other Me−Pt signals (δ 0.38, ^2J(PtH) = 72.4 Hz; δ 1.45, ^2J(PtH) = 70.7 Hz) with the high-frequency signal having twice the intensity of the low-frequency signal. These resonances are due to [$PtMe_3Cl(bpy)$],[8] the product of α-elimination of dimethylstannylene, Me_2Sn, from [$PtClMe_2(Me_3Sn)(bpy)$]. A ^{1}H NMR analysis of the volatile products of decomposition shows both Me_3SnCl (δ 0.58) and Me_4Sn (δ 0.05) to be present along with a number of minor unidentified products. These unidentified volatiles are likely products of indiscriminate reactions of the unstable Me_2Sn. Similar pyrolysis experiments have been carried out on a number of other platinum(IV) complexes, and the results are summarized in Table 2.

DSC Studies of Platinum(IV) Complexes: Determination of the Pt−Si Bond Energy in [$PtIMe_2(Me_3Si)(bpy)$]. DSC results for the first decomposition step of a series of platinum(IV) complexes are presented in Table 3. In many cases there are several close or overlapping signals, indicating multiple decomposition pathways over a small temperature range. This is in accord with the TGA and ^{1}H NMR results presented above. Due to the complexity of most DSC results, analysis of reaction thermodynamics is not straightforward or practical. For this reason we have concentrated our efforts on the decomposition of complexes of the type [$PtIMe_2(Me_3Si)$(diimine)], as we have shown these species to decompose almost entirely by a single pathway (Me_4Si elimination). The production of a single, nonreactive volatile component is well suited to thermodynamic analysis of the reaction by DSC. The clean decomposition of [$PtIMe_2(Me_3Si)(bpy)$] allows for a straightforward estimation of the Pt−Si bond dissociation energy through the use of DSC. The enthalpy of a reaction can be approximated as the difference in dissociation energies between the bond formed and bonds broken. For the decomposition of [$PtIMe_2(Me_3Si)(bpy)$] this gives rise to eq 1, from which D(Pt−$SiMe_3$)

$$\Delta H_{rxn} = D(\text{Pt}-\text{CH}_3) + D(\text{Pt}-\text{SiMe}_3) - D(\text{Me}_3\text{Si}-\text{Me}) \quad (1)$$

can be estimated, though several approximations and assumptions are necessary.[9] This is why we consider this an estimate rather than a determination of D(Pt-Si).

Figure 3 shows the DSC result for the decomposition of [$PtIMe_2(Me_3Si)(bpy)$]. Decomposition occurs over the range 177−195 °C, corresponding closely to the 172−194 °C range observed by TGA for the same process. The signal shows exothermic and endothermic regions. This can be accounted for in terms of an exothermic reaction which is accompanied by an endothermic transition, partially due to the phase transition of the solid and, perhaps, partially due to volatilization of Me_4-Si. The heat of reaction was determined to be -8 ± 5 kJ/mol from eight experiments.

Discussion

Inspection of the TGA data reveals a number of trends. The thermal stability of complexes varies, depending on the diimine ligand, in the order bpy > bpy-$^tbu_2$ > paen-me_2 > py-*n*-pr, likely the result of packing effects, since no substantial electronic differences are expected. Stability also varies according to the group 14 element, Sn ≈ Ge > Si, in accordance with the results of previous studies.[10] There is also a clear trend for increased thermal stability with increased halide size (Figure 2). In most cases, the TGA results are not consistent with a single mode of decomposition, as indicated by the theoretical mass losses presented in Table 1. Despite the fact that specific decomposition modes cannot generally be established from the TGA

(7) Clark, H. C.; Manzer, L. E. *J. Organomet. Chem.* **1973**, *59*, 411.
(8) Kuyper, J. *Inorg. Chem.* **1978**, *17*, 77.

(9) There are a number of approximations made in this type of treatment. The energies of bonds that are not directly involved in the reaction are assumed to remain constant, and no account of the Pt(IV)−Pt(II) promotional energy is made. Note that in the present case it is necessary to assume that the remaining Pt−C, Pt−N, and Pt−I bond dissociation energies are the same as in the Pt(IV) precursors and that the heats of sublimation of precursor and product are the same. As well, there are a number of difficulties associated with the practical aspects of DSC. For a discussion, see: MacKenzie, R. C. *Differential Thermal Analysis*; Academic Press: New York, 1970; Vol. 1, pp 55−120.

(10) Hartley, F. R. *The Chemistry of Platinum and Palladium*; Applied Science: London, 1973; p 81.

Table 1. TGA Data for the First Decomposition Step of Complexes of the Type [PtMe$_2$(Me$_3$E)X(diimine)] (E = Sn, Ge, X = Cl, Br, I; Si, X = Br, I)

diimine ligand	Me_3EX	onset temp (°C)	final temp (°C)	1st mass loss (%)	theor Me_3EX[a] (%)	theor Me_4E[b] (%)	theor Me_2E[c] (%)
bpy	Me_3SnCl	147	180	29.2	34.3	30.8	25.6
bpy	Me_3SnBr	166	215	33.8	39.0	28.6	23.8
bpy	Me_3SnI	171	217	33.3	50.0	30.7	25.5
bpy	Me_3SiBr	161	176	24.4	28.7	16.5	13.7
bpy	Me_3SiI	172	194	18.7	34.4	15.2	12.6
bpy-^{t}bu$_2$	Me_3SnCl[d]	145	165	42.7	44.7[e]	42.4[f]	39.0[g]
bpy-^{t}bu$_2$	Me_3SnBr[d]	147	176	45.6	49.7[e]	43.1[f]	40.0[g]
bpy-^{t}bu$_2$	Me_3SnI[d]	149	192	35.9	54.1[e]	43.7[f]	40.9[g]
bpy-^{t}bu$_2$	Me_3GeCl	131	165	21.6	23.7	20.5	15.9
bpy-^{t}bu$_2$	Me_3GeBr	140	176	28.5	28.6	19.2	14.9
bpy-^{t}bu$_2$	Me_3GeI	140	226	28.9	33.1	18.0	13.9
bpy-^{t}bu$_2$	Me_3SiBr	117	131	17.1	23.7	13.6	9.0
bpy-^{t}bu$_2$	Me_3SiI	127	167	17.2	28.9	12.7	8.4
py-*n*-pr	Me_3SnCl	82	199	28.7	30.0	26.9	22.4
py-*n*-pr	Me_3SnBr	98	150	23.4	39.5	29.0	24.1
py-*n*-pr	Me_3SnI	91	161	20.7	43.7	26.9	22.4
py-*n*-pr	Me_3SiBr	116	141	23.3	29.1	16.8	11.1
py-*n*-pr	Me_3SiI	139	158	16.1	34.9	15.4	10.1
paen-me$_2$	Me_3SnCl	116	162	26.4	33.1	29.7	24.7
paen-me$_2$	Me_3SnBr	136	181	35.6	37.7	27.7	23.0
paen-me$_2$	Me_3SnI	153	183	30.1	41.9	25.8	21.5
paen-me$_2$	Me_3SiBr	114	127	21.7	27.6	15.9	10.5
paen-me$_2$	Me_3SiI	136	157	15.3	33.2	14.6	9.6

[a] Theoretical mass change upon loss of Me_3EX. [b] Theoretical mass change upon loss of Me_4E. [c] Theoretical mass change upon loss of Me_2E. [d] Compelx has formula [PtMe$_2$X(Me$_3$Sn)(bpy-^{t}bu$_2$)]·Me$_3$SnX. [e] Theoretical mass change upon loss of two molecules of Me_3SnX. [f] Theoretical mass change upon loss of one molecule each of Me_3SnX and Me_4Sn. [g] Theoretical mass change upon loss of one molecule each of Me_3SnX and Me_2Sn.

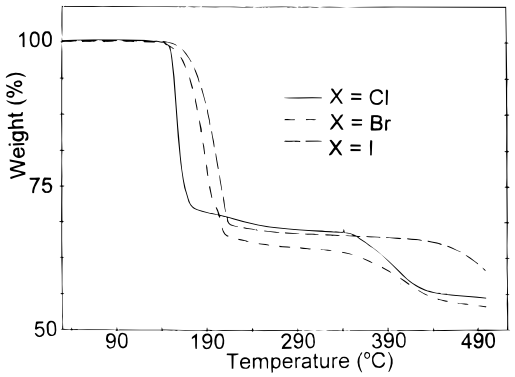

Figure 2. TGA curves of [PtXMe$_2$(Me$_3$Sn)(bpy)] (X = Cl, Br, I).

Table 2. Decomposition Products of Platinum(IV) Complexes

platinum(IV) complex	[PtMe$_2$ (N−N) (%)	[PtMeX (N−N)] (%)	[PtMe$_3$X (N−N)] (%)
[PtClMe$_2$(Me$_3$Sn)(bpy)]	51	26	23
[PtBrMe$_2$(Me$_3$Sn)(bpy)]	M[a]	m[b]	m
[PtIMe$_2$(Me$_3$Sn)(bpy)]	∼0	∼0	∼100
[PtClMe$_2$(Me$_3$Ge)(bpy-^{t}bu$_2$)]	37	54	9
[PtBrMe$_2$(Me$_3$Ge)(bpy-^{t}bu$_2$)]	50	50	∼0
[PtIMe$_2$(Me$_3$Ge)(bpy-^{t}bu$_2$)]	10	90	∼0
[PtBrMe$_2$(Me$_3$Si)(bpy)][c]	41	59	∼0
[PtBrMe$_2$(Me$_3$Si)(bpy)][d]	64	36	∼0
[PtIMe$_2$(Me$_3$Si)(bpy)]	3	97	∼0

[a] Major product. [b] Minor product. [c] 190 °C. [d] 210 °C.

data, certain trends are evident and are confirmed by NMR studies of pyrolysis products. The degree of decomposition resulting from Me_4E and Me_2E elimination generally increases with increasing halide size, and there is a corresponding decrease in the reductive elimination of Me_3EX. This may be a result of the increasing difficulty in breaking the Pt−X bond in the order Cl < Br < I, as evidenced by the higher onset temperatures in the same series.

TGA results along with NMR studies of pyrolysis products indicate three decomposition pathways for [PtClMe$_2$(Me$_3$Sn)(bpy)] (Scheme 1).[11] The decomposition pattern of [PtClMe$_2$(Me$_3$Sn)(bpy)] has features similar to those reported for other platinum complexes. Decomposition by the competitive reductive elimination of Me_3SnCl and Me_4Sn is analogous to that observed for the thermolysis of [PtIMe$_3$(dppe)], which undergoes reductive elimination of C_2H_6 (82%) and MeI (18%).[4] In this case, reductive elimination of ethane is the major decomposition pathway, while for [PtClMe$_2$(Me$_3$Sn)(bpy)] the corresponding reductive elimination of tetramethyltin is only a minor pathway. The third decomposition pathway for [PtClMe$_2$(Me$_3$Sn)(bpy)] is the elimination of Me_2Sn, a process which is not a reductive elimination and gives a platinum(IV) product. Similar eliminations of germylene and silylene fragments have been observed by Tanaka and co-workers[12,13] for certain platinum(II) complexes, but in these cases the platinum center was coordinatively unsaturated.

From a mechanistic viewpoint, it is likely that the first step in thermolysis is the dissociation of the Pt−X bond, as illustrated for the thermolysis of [PtClMe$_2$(Me$_3$Sn)(bpy)] in Scheme 2.[4,14,15] The reductive elimination of Me_3SnCl from [PtClMe$_2$(Me$_3$Sn)(bpy)] presumably occurs by a mechanism which is the reverse of the S_N2 process. This is a very rapid, reversible process in solution[16] but is clearly much slower in the solid-state thermolysis, probably because the chloride ion cannot easily migrate from platinum, as required (Scheme 2,

(11) The percentages given in Scheme 1 represent product ratios of complexes in solution. It must be noted that there was a small amount of insoluble material resulting from decomposition.

(12) Kobayashi, T.; Hayashi, T; Yamashita, H.; Tanaka, M. *Chem. Lett.* **1988**, 1411.

(13) Yamashita, H.; Kobayashi, T.; Tanaka, M.; Samuels, J. A.; Streib, W. E. *Organometallics* **1992**, *11*, 2330.

(14) Roy, S.; Puddephatt, R. J.; Scott, J. D. *J. Chem. Soc., Dalton Trans.* **1989**, 2121.

(15) Brown, M. P.; Puddephatt, R. J.; Upton, J. *J. Chem. Soc., Dalton Trans.* **1974**, 2457.

(16) Levy, C. J.; Puddephatt, R. J. *J. Chem. Soc., Chem. Commun.* **1995**, 2115.

Table 3. DSC Signals for Platinum(IV) Compelxes[a]

complex	T_1 (°C)	T_3 (°C)	T_3 (°C)	T_4 (°C)
$[PtClMe_2(Me_3Sn)(bpy\text{-}^tbu_2)]\cdot Me_3SnCl$	161, ex	172, en	176, ex	
$[PtBrMe_2(Me_3Sn)(bpy\text{-}^tbu_2)]\cdot Me_3SnBr$	173, ex	186, en	192, ex	197, ex
$[PtIMe_2(Me_3Sn)(bpy\text{-}^tbu_2)]\cdot Me_3SnI$	174, ex	188, en	198, ex	
$[PtBrMe_2(Me_3Si)(bpy\text{-}^tbu_2)]$	103, ex	115, ex	120, en	135, ex
$[PtIMe_2(Me_3Si)(bpy\text{-}^tbu_2)]$	134, ex	169, ex		
$[PtBrMe_2(Me_3Si)(bpy)]$	169, en	174, ex		
$[PtIMe_2(Me_3Si)(bpy)]$	187, en	192, ex		
$[PtIMe_2(Me_3Si)(py\text{-}n\text{-}pr)]$	147, ex	153, en		
$[PtIMe_2(Me_3Si)(paen\text{-}me_2)]$	137, ex	152, ex	165, ex	

[a] T_1-T_4 are labels for DSC signals (in terms of increasing temperature) arising from initial decomposition of the platinum(IV) complexes. The terms en and ex indicate endothermic and exothermic signals, respectively.

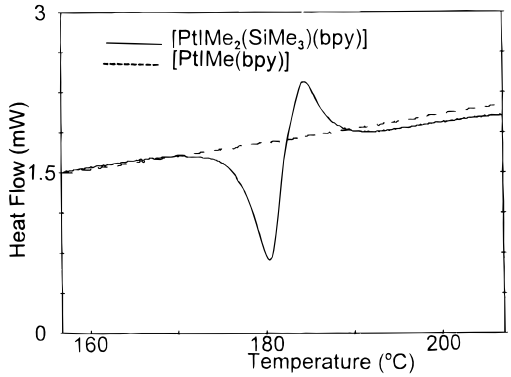

Figure 3. DSC signal for the reductive elimination of Me_4Si from $[PtIMe_2(Me_3Si)(bpy)]$. Conditions: scan rate, 10.0 °C min^{-1}; sample weight, 1.477 mg; area, −8.9 J g^{-1} (=−5.2 kJ mol^{-1}).

Scheme 1

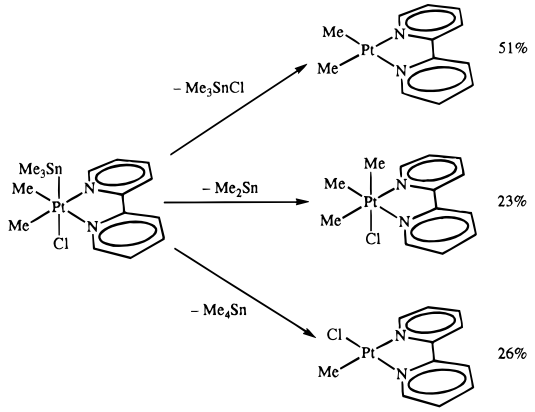

route A). Such a pathway is rare for alkylplatinum(IV) complexes.[1] The elimination of Me_4Sn probably follows the more common mode of reductive elimination from Pt(IV) complexes, namely a concerted 1, 1-reductive elimination (Scheme 2, route B). The elimination of Me_2Sn from $[PtClMe_2(Me_3Sn)(bpy)]$ requires methyl group transfer from the trimethyltin ligand to the platinum center along with Pt−Sn bond cleavage. Because the platinum(IV) center is coordinatively saturated, it seems unlikely that this occurs directly. One possible mechanism involves dissociation of the chloro ligand followed by α-migration of a methyl group from the tin to the platinum center with concomitant elimination of Me_2Sn, then followed by displacement of "Me_2Sn" by Cl^- (Scheme 2, route C). The strong *trans* effect of the Me_3Sn ligand makes the Pt−Cl bond relatively easy to cleave.

Our studies of silyl- and germylplatinum(IV) complexes show that Me_4E (E = Si, Ge) elimination is

Scheme 2

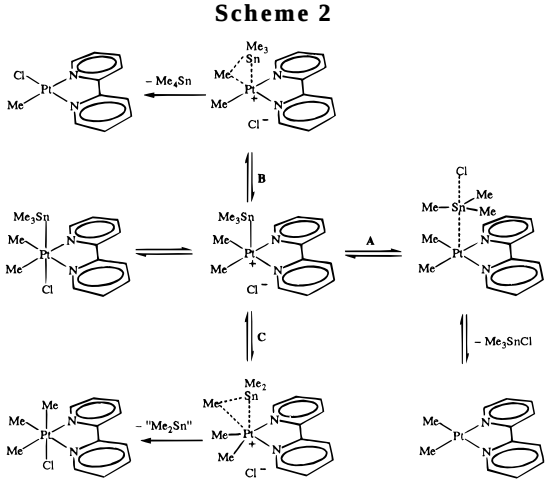

favored in the order Cl < Br < I, with a corresponding decrease in reductive elimination of Me_3EX (E = Si, Ge). The decrease in Me_3EX with increasing halide size is consistent with the results obtained for similar platinum(IV)−tin complexes. The germanium complexes do not show significant decomposition by the elimination of Me_2Ge. This is only a minor pathway for the chloro complex, and it is not observed for the bromo and iodo complexes. Silylplatinum(IV) complexes do not show any decomposition *via* the elimination of Me_2Si. These results are in contrast to those obtained for the platinum(IV)−tin complexes, which show an increasing degree of decomposition by this pathway in the order Cl < Br < I. The decrease in decomposition by the elimination of Me_2E in the series Sn > Ge > Si is consistent with the clear trend of decreased E−Me bond dissociation energies in the order E = C > Si > Ge > Sn.[17] Average E−Me bond energies for Me_4E are 317, 265, and 226 kJ/mol for E = Si, Ge, and Sn, respectively.

The pyrolyses of $[PtBrMe_2(Me_3Si)(bpy)]$ at 190 and 210 °C clearly show an increased proportion of decomposition by Me_3SiBr reductive elimination with increased temperature and indicates higher activation barrier for this process than for the reductive elimination of Me_4Si.

DSC studies have provided the first experimental estimation of a Pt−Si bond energy. Literature values for *D*(Me−Pt) and *D*(Me−Si) were required for this analysis. The Me_3Si−Me bond energy has been derived by Walsh[17] to be 376 ± 8 kJ mol^{-1}. Several literature values are available for the Me−Pt(IV) bond dissociation energy. A value of 134 kJ mol^{-1} is predicted by the

(17) Walsh, R. In *The Chemistry of Organic Silicon Compounds*; Patai, S., Rappaport, Z., Eds.; Wiley: Toronto, 1989; p 376−385.

generalized valence bond theory for $[PtCl_2Me_2(PH_3)_2]$,[18] values of 137 and 125 kJ mol^{-1} have been found for *cis*-$[PtMe_4L_2]$ (L = MeCN, 2,6-$Me_2C_6H_3NC$),[14] a value of 144 kJ mol^{-1} was found for $[PtIMe_3(PMe_2Ph)_2]$,[15] and a value of 132 kJ mol^{-1} was determined for $[PtIMe_3(dppe)]$ (dppe = $Ph_2PCH_2CH_2PPh_2$).[3b] We have used an average of the experimentally determined bond dissociation energies (135 ± 10 kJ mol^{-1})[19] for our calculations. Using the literature bond dissociation energy data, we obtain an estimated value for D(Pt−$SiMe_3$) in $[PtIMe_2(Me_3Si)(bpy)]$ of 233 ± 14 kJ mol^{-1}. This is 98 kJ mol^{-1} larger than the D(Pt−Me) value used in our calculations, clearly showing the stronger nature of the Pt−Si bonding interaction compared to Pt−Me. This result is consistent with the general stability trend Pt−Si > Pt−C.[20]

Literature data on transition-metal−group 14 bond energies are sparse.[5] Beauchamp and co-workers[21] have determined TM−Si bond energies for metal ion-silylene complexes in the gas phase. The Ni−Si bond energy in $[Ni{=}SiH_2]^+$ was found to be 280 ± 25 kJ mol^{-1}. Sakaki and Ieki[22] have used *ab initio* calculations to estimate D(Pt−SiH_3) values for simple platinum(II)−phosphine complexes. These authors obtained values which range from 249 to 269 kJ mol^{-1}, compared to 165−177 kJ mol^{-1} for D(Pt−Me) in these model complexes. The calculated Pt−Si bond lengths associated with these bond energies are in the range 2.366−2.399 Å, similar to the 2.337(3) Å found for $[PtIMe_2(Me_3Si)(bpy)]$.[23] The value of D(Pt−Si) obtained for $[PtIMe_2(Me_3Si)(bpy)]$ (233 kJ mol^{-1}) agrees well with those obtained from the *ab initio* calculations, and both studies indicate a Pt−Si bond which is approximately 100 kJ mol^{-1} stronger than the Pt−CH_3 bond. An extensive chemistry of silylplatinum complexes can therefore be anticipated.[24]

Conclusions

TGA studies show increased stability for $[PtX(Me_3E)Me_2(diimine)]$ complexes in the order X = Cl < Br < I and E = Si ≈ Ge < Sn. TGA and ^{1}H NMR studies of the decomposition of platinum(IV) complexes indicate that there are up to three competitive decomposition processes: 1,1-reductive elimination of Me_4E, reductive elimination of Me_3EX, and α-elimination of Me_2E. The generation of Me_2Sn and Me_2Ge from platinum(IV) complexes has no precedent in organoplatinum(IV) complexes. We attribute this to the increasing Me−E bond dissociation energies in the order Sn < Ge < Si < C, which makes transfer of a methyl group from the group 14 element to platinum more difficult with lighter group 14 elements. The reductive elimination of Me_3EX from many platinum(IV) complexes studied in this work is in agreement with the observed trend that *trans* RX reductive elimination is predominant when a ligand of strong *trans* effect is *trans* to the eliminated halide.[2,3b]

For the first time we have experimentally estimated a Pt−Si bond dissociation energy. This value of the Pt−Si bond energy, while approximate, has obvious relevance to catalytic processes, such as hydrosilylation, which involve the making and breaking of Pt−Si bonds. As well, new bond energy data are valuable for the prediction of reaction thermodynamics and reaction feasibility. Our DSC results give a D(Pt−$SiMe_3$) value of 233 ± 14 kJ mol^{-1} for $[PtIMe_2(Me_3Si)(bpy)]$. This is considerably larger (∼100 kJ mol^{-1}) than for the Pt^{IV}−CH_3 bond, demonstrating the dramatic increase in Pt−E (E = C, Si, Ge, Sn) bond energy on going to softer group 14 elements.

Experimental Section

DSC experiments were conducted using a Perkin-Elmer DSC7 with a TAC7/DX thermal analysis controller. Samples were weighed into empty aluminum pans, with the weight of each (0.5−3 mg) being determined using a microbalance (supplied with the Perkin-Elmer TGA7). Pans were not sealed in order to allow for the escape of volatile products.[15] The sample and reference compartments were purged with N_2 during the experiments. Scan rates of 5−20 °C/min were used. Thermogravimetric analysis (TGA) experiments were conducted using a Perkin-Elmer TGA7 with a TAC7/DX thermal analysis controller. Dry samples were weighed (1−4 mg) into a platinum pan and were heated at 15−20 °C/min under a stream of N_2. All pyrolysis experiments were carried out in NMR tubes which were fitted with J. Young valves (Aldrich Catalog No. Z18,397-0) and could be sealed under vacuum. Dry platinum(IV) complexes (*ca.* 10 mg) in evacuated NMR tubes were heated for 20 min in a temperature-controlled oil bath. Integrals for ^{1}H NMR signals are assigned with respect to the major Me−Pt signal. The ^{1}H NMR parameters for $[PtXMe_3(bpy)]$ (X = Br, I) have been previously reported.[8,25]

Pyrolysis of $[PtClMe_2(Me_3Sn)(bpy)]$. Two samples of $[PtClMe_2(Me_3Sn)(bpy)]$ were heated at 190 °C in NMR tubes. The solid darkened from yellow to brown, and colorless crystals were formed on the sides of the NMR tubes (above the level of the oil bath). A N_2 atmosphere was introduced into one tube, and acetone-d_6 was then added. The other tube was placed under dynamic vacuum to remove any volatile material, and the residue was dissolved in acetone-d_6. Both tubes contained yellow solutions along with dark insoluble material. The ^{1}H NMR spectrum (acetone-d_6) of the solid residue with volatiles removed was consistent with a mixture of 51% $[PtMe_2(bpy)]$, 26% [PtClMe(bpy)], and 23% $[PtClMe_3(bpy)]$. Methyl−platinum signals were as follows: $[PtMe_2(bpy)]$ δ 0.97 [s, ^2J(PtH) = 86.1 Hz]; [PtClMe(bpy)] δ 1.05 [s, ^2J(PtH) = 79.2 Hz]; $[PtClMe_3(bpy)]$ δ 0.37 [s, 3H, ^2J(PtH) = 74.1 Hz, axial Me], δ 1.22 [s, 6H, ^2J(PtH) = 70.2 Hz, equatorial Me]. The ^{1}H NMR spectrum (acetone-d_6) of the solid residue in the presence of volatiles is very similar, with two extra signals, corresponding to an 11:89 ratio of Me_4Sn:Me_3SnCl: Me_4Sn δ 0.05 [s, $^2J(SnH)_{av}$ = 54 Hz]; Me_3SnCl δ 0.58 [s, $^2J(^{119}SnH)$ = 64.9 Hz, $^2J(^{117}SnH)$ = 62.2 Hz]. The aromatic region of both spectra is complicated, with overlapping signals arising from the three major platinum products. The same procedure was followed for the pyrolyses of $[PtBrMe_2(Me_3Sn)(bpy)]$ and $[PtIMe_2(Me_3Sn)(bpy)]$, except that the oil bath temperature was maintained at 220 °C for

(18) Low, J. J.; Goddard, W. A., III. *J. Am. Chem. Soc.* **1986**, *108*, 6115.
(19) The error is estimated from the spread of the literature bond energy data.
(20) McKay, K. M.; Nicholson, B. K. In *Comprehensive Organometallic Chemistry*, Wilkinson, G., Stone, F. G. A., Abel, E. W., Eds.; Pergamon: Oxford, U.K., 1982; Vol. 6, pp 1096−1097.
(21) Kang, H.; Jacobson, D. B.; Shin, S. K.; Beauchamp, J. L.; Bowers, M. T. *J. Am. Chem. Soc.* **1986**, *108*, 5668.
(22) Sakaki, S.; Ieki, M. *J. Am. Chem. Soc.* **1993**, *115*, 2373.
(23) Levy, C. J.; Vittal, J. J.; Puddephatt, R. J. *Organometallics* **1994**, *13*, 1559.
(24) (a) Heyn, R. H.; Tilley, T. D. *J. Am. Chem. Soc.* **1992**, *114*, 1917. (b) Chang, L. S.; Johnson, M. P.; Fink, M. J. *Organometallics* **1991**, *10*, 1219. (c) Grumbine, S. D.; Tilley, T. D.; Arnold, F. P.; Rheingold, A. L. *J. Am. Chem. Soc.* **1993**, *115*, 7884. (d) Latif, L. A.; Eaborn, C.; Pidcock, A.; Weng, N. S. *J. Organomet. Chem.* **1994**, *474*, 217. (e) Ozawa, F.; Hikida, T.; Hayashi, T. *J. Am. Chem. Soc.* **1994**, *116*, 2844. (f) Yamashita, H.; Kobayashi, T.; Hayashi, T.; Tanaka, M. *Chem. Lett.* **1990**, 1447. (g) Yamashita, H.; Tanaka, M.; Goto, M. *Organometallics* **1992**, *11*, 3227. (h) Yamashita, H.; Tanaka, M.; Goto, M. *Organometallics* **1993**, *12*, 988.
(25) Crespo, M.; Puddephatt, R. J. *Organometallics* **1987**, *6*, 2548.

the former and 230 °C for the latter. For the decomposition of [$PtBrMe_2(Me_3Sn)(bpy)$], the ^1H NMR spectrum (acetone-d_6) of the solid with volatiles removed is consistent with a mixture of [$PtBrMe_2(Me_3Sn)(bpy)$] (not decomposed), [$PtMe_2(bpy)$] (major product), and [$PtBrMe_3(bpy)$] (minor product). Signals due to Me−Pt were as follows: [$PtBrMe_2(Me_3Sn)(bpy)$] and [$PtMe_2(bpy)$] (equilibrium mixture) δ 1.05 [s (br), $^2J(PtH) = 80.5$ Hz]; [$PtBrMe_3(bpy)$] δ 0.46 [s, 3H, $^2J(PtH) = 74.2$ Hz], δ 1.31 [s, 6H, $^2J(PtH) = 70$ Hz]. The ^1H NMR spectrum (acetone-d_6) of the solid in the presence of volatiles indicates a Me_3SnBr:Me_4Sn ratio of 86:14. ^1H NMR spectra of volatiles: δ 0.05 [s, $^2J(SnH)_{av} = 54$ Hz, Me_4Sn], δ 0.15 [s, unidentified volatile], δ 0.60 [s (br), $^2J(SnH)_{av} = 61$ Hz, averaged Me_3Sn signal]. For the decomposition of [$PtIMe_2(Me_3Sn)(bpy)$], the ^1H NMR spectrum (acetone-d_6) of the residue with volatiles removed is consistent with a mixture of [$PtIMe_2(Me_3Sn)(bpy)$] (not decomposed), [$PtIMe_3(bpy)$], and [PtIMe(bpy)]. The relative percentages of [$PtIMe_3(bpy)$] and [PtIMe(bpy)] are 93% and 7%, respectively. Signals due to Me−Pt and Me−Sn were as follows: [$PtIMe_2(Me_3Sn)(bpy)$] δ −0.20 [s(br), 9H, Me−Sn], δ 1.43 [s (br), 6H, $^2J(PtH) = 64.8$ Hz, Me−Pt]; [$PtIMe_3(bpy)$] δ 0.57 [s, 3H, $^2J(PtH) = 72.4$ Hz, axial Me−Pt], δ 1.45 [s, 6H, $^2J(PtH) = 70.7$ Hz, equatorial Me−Pt]; [PtIMe(bpy)] δ 1.27 [s, $^2J(PtH)$ unresolved]. The ^1H NMR spectrum of the solid in the presence of volatiles indicates that Me_4Sn is the major volatile component, with a minor signal due to an unidentified compound (intensity of 17% with respect to the Me_4Sn signal).

Pyrolysis of [$PtBrMe_2(Me_3Si)(bpy)$]. A sample of [$PtBrMe_2(Me_3Si)(bpy)$] was heated in an oil bath at 210 °C. The solid darkened from yellow to brown-yellow. The tube was attached to a vacuum manifold, and the volatile components were distilled into a second NMR tube. CD_2Cl_2 was distilled into each tube by vacuum transfer. The solution of the solid residue was yellow, with a small amount of dark solid. ^1H NMR spectrum (CD_2Cl_2) of the solid, with volatiles removed, shows signals due to [$PtMe_2(bpy)$], [PtBrMe(bpy)], and a small amount of [$PtBrMe_2(Me_3Si)(bpy)$] (not decomposed). The [$PtMe_2(bpy)$]:[PtBrMe(bpy)] ratio is 41:59. Signals due to Me−Pt were as follows: [$PtMe_2(bpy)$] δ 0.99 [s, $^2J(PtH) = 85.5$ Hz]; [PtBrMe(bpy)] δ 1.14 [s, $^2J(PtH) = 79.6$ Hz]. The ^1H NMR spectrum (CD_2Cl_2) of the volatile products shows Me_4Si (δ 0.00), as well as a number of other unidentified resonances (δ 0.07, 0.13, 0.21). Pyrolysis at 190 °C was carried out using the same procedure as at 210 °C. Similar results were obtained, except that the [$PtMe_2(bpy)$]:[PtBrMe(bpy)] ratio had increased from 41:59 (210 °C) to 64:36. The pyrolyses of [$PtIMe_2(Me_3Si)(bpy)$] and [$PtClMe_2(Me_3Ge)(bpy\text{-}^tbu_2)$] (X = Cl, Br, I) were carried out. [$PtIMe_2(Me_3Si)(bpy)$] was pyrolyzed at 155 °C. The ^1H NMR spectrum (CD_2Cl_2) of the solid residue shows [$PtIMe_2(Me_3Si)(bpy)$] (not decomposed) as well as [PtIMe(bpy)] and [$PtMe_2(bpy)$]. The [PtIMe(bpy)]:[$PtMe_2(bpy)$] ratio was 97:3. Signals due to Me−Pt and Me−Si were as follows: [$PtIMe_2(Me_3Si)(bpy)$] δ −0.33 [s, 9H, $^3J(PtH) = 19.0$ Hz, Me−Si], δ 1.45 [s, 6H, $^2J(PtH) = 64.3$ Hz, Me−Pt]; [PtIMe(bpy)] δ 1.15 [s, 6H, $^2J(PtH) = 75.8$ Hz, Me−Pt]; δ 0.98 [s, $^2J(PtH) = 86.1$ Hz, Me−Pt]. The ^1H NMR spectrum of the volatiles (C_6D_6) showed predominantly Me_4Si (δ 0.00) as well as a minor signal at 0.10 ppm (5% intensity compared to the Me_4Si resonance) which is not, as yet, assigned. [$PtClMe_2(Me_3Ge)(bpy\text{-}^tbu_2)$] was pyrolyzed at 210 °C. The ^1H NMR spectrum (CD_2Cl_2) of the solid shows a 37:54:9 mixture of [$PtMe_2(bpy\text{-}^tbu_2)$]:[$PtClMe(bpy\text{-}^tbu_2)$]:[$PtClMe_3(bpy\text{-}^tbu_2)$], respectively: [$PtMe_2(bpy\text{-}^tbu_2)$] δ 0.92 [s, $^2J(PtH) = 85.4$ Hz, Me−Pt]; [$PtClMe(bpy\text{-}^tbu_2)$] δ 1.05 [s, $^2J(PtH) = 78.4$ Hz, Me-Pt]; [$PtClMe_3(bpy\text{-}^tbu_2)$] δ 0.39 [s, 3H, $^2J(PtH) = 75.5$ Hz, axial Me−Pt], δ 1.22 [s, 6H, $^2J(PtH) = 69.5$ Hz, equatorial Me−Pt]. The ^1H NMR spectrum of the volatiles (C_6D_6) shows signals due to Me_3GeCl and Me_4Ge, as well as two unidentified compounds: δ 0.17 [s, Me_4Ge], δ 0.31 [s, unidentified volatile], δ 0.36 [s, Me_3GeCl], δ 0.40 [s, unidentified volatile]. [$PtBrMe_2(Me_3Ge)(bpy\text{-}^tbu_2)$] was pyrolyzed at 210 °C. The ^1H NMR spectrum (CD_2Cl_2) of the solid showed [$PtBrMe_2(Me_3Ge)(bpy\text{-}^tbu_2)$] (not decomposed), [$PtMe_2(bpy\text{-}^tbu_2)$], and [$PtBrMe(bpy\text{-}^tbu_2)$]. The ratio [$PtMe_2(bpy\text{-}^tbu_2)$]:[$PtBrMe(bpy\text{-}^tbu_2)$] was 1:1. Signals due to Me−Pt and Me−Ge were as follows: [$PtBrMe_2(Me_3Ge)(bpy\text{-}^tbu_2)$] δ −0.22 [s, $^2J(PtH) = 17.7$ Hz, Me−Ge], δ 1.28 [s, $^2J(PtH) = 63.3$ Hz, Me−Pt]; [$PtMe_2(bpy\text{-}^tbu_2)$] δ 0.92 [s, $^2J(PtH) = 85.4$ Hz, Me−Pt]; [$PtBrMe(bpy\text{-}^tbu_2)$] δ 1.08 [s, $^2J(PtH) = 76.8$ Hz, Me−Pt]. The ^1H NMR spectrum (C_6D_6) of the volatiles shows essentially pure Me_3GeBr (δ 0.48). [$PtIMe_2(Me_3Ge)(bpy\text{-}^tbu_2)$] was pyrolyzed at 230 °C. The ^1H NMR spectrum (CD_2Cl_2) of the solid showed [$PtIMe_2(Me_3Ge)(bpy\text{-}^tbu_2)$] (not decomposed), [$PtIMe(bpy\text{-}^tbu_2)$], and [$PtMe_2(bpy\text{-}^tbu_2)$]. The ratio [$PtIMe(bpy\text{-}^tbu_2)$]:[$PtMe_2(bpy\text{-}^tbu_2)$] was 9:1. Signals due to Me−Pt and Me−Ge were as follows: [$PtIMe_2(Me_3Ge)(bpy\text{-}^tbu_2)$] δ −0.28 [s, 9H, $^3J(PtH) = 18.0$ Hz, Me−Ge], δ 1.44 [s, 6H, $^2J(PtH) = 64.2$ Hz, Me−Pt]; [PtIMe(bpy-^{t}bu$_2$)] δ 1.11 [s, $^2J(PtH) = 76.1$ Hz, Me−Pt]; [$PtMe_2(bpy\text{-}^tbu_2)$] δ 0.92 [s, $^2J(PtH) = 85.4$ Hz, Me−Pt]. The ^1H NMR spectrum (C_6D_6) of the volatiles shows Me_3GeI (δ 0.64) and Me_4Ge (δ 0.12) to be the major components. Signals of lesser intensity are observed at δ 0.31, 0.36, and 0.40.

Pyrolysis of [$PtClMe_2(Me_3Sn)(bpy\text{-}^tbu_2)$]·$Me_3SnCl$. [$PtClMe_2(Me_3Sn)(bpy\text{-}^tbu_2)$]·$Me_3SnCl$ was heated at 175 °C, and the solid changed from light yellow to orange. A colorless solid formed in the tube above the level of the oil bath. The tube was attached to a vacuum manifold, and the volatiles were vacuum-transferred to a second NMR tube. The tubes were placed under an atmosphere of nitrogen, and acetone-d_6 was added to both. The ^1H NMR spectrum (acetone-d_6) of the solid residue shows a mixture of [$PtClMe_2(Me_3Sn)(bpy\text{-}^tbu_2)$], [$PtMe_2(bpy\text{-}^tbu_2)$], [$PtClMe(bpy\text{-}^tbu_2)$], and [$PtClMe_3(bpy\text{-}^tbu_2)$]. [$PtClMe_2(Me_3Sn)(bpy\text{-}^tbu_2)$] and [$PtMe_2(bpy\text{-}^tbu_2)$] show averaged signals due to rapid exchange. Integration shows the following relative percentages of decomposition products: [$PtMe_2(bpy\text{-}^tbu_2)$], 58%; [$PtClMe(bpy\text{-}^tbu_2)$], 24%; [$PtClMe_3(bpy\text{-}^tbu_2)$], 18%. Signals due to Me−Pt were as follows: [$PtMe_2(bpy\text{-}^tbu_2)$] δ 0.93 [s, $^2J(PtH) = 83.7$ Hz, Me−Pt]; [$PtClMe(bpy\text{-}^tbu_2)$] δ 0.99 [s, $^2J(PtH) = 78.4$ Hz, Me−Pt]; [$PtClMe_3(bpy\text{-}^tbu_2)$] δ 0.36 [s, 3H, $^2J(PtH)$ is unresolved, axial Me−Pt], δ 1.19 [s, 6H, $^2J(PtH) = 70.6$ Hz, equatorial Me−Pt]. The ^1H NMR spectrum (acetone-d_6) of the volatile components shows a 95:5 ratio of Me_3SnCl:Me_4Sn: δ 0.05 [s, $^2J(SnH)_{av} = 52.9$ Hz, Me_4Sn]; δ 0.61 [s, $^2J(SnH)_{av} = 63.5$ Hz, Me_3SnCl]. The pyrolysis of [$PtBrMe_2(Me_3Sn)(bpy\text{-}^tbu_2)$]·$Me_3SnBr$ was carried out using the same procedure, except that the oil bath was maintained at 185 °C. The ^1H NMR spectrum (acetone-d_6) of the solid residue in acetone-d_6 (orange solution and orange solid) corresponds to that of [$PtBrMe_2(Me_3Sn)(bpy\text{-}^tbu_2)$]: δ 0.41 [s (v br), 9H, Me−Sn], δ 0.94 [s, 6H, $^2J(PtH) = 83.7$ Hz, Me−Pt], δ 1.43 [s, 18H, ^{t}bu], δ 7.80 [dd, $^2J(H^aH^b) = 6.3$ Hz, $^3J(H^bH^d) = 2.1$ Hz, H^b], δ 8.61 [d, 2H, H^d], δ 8.90 [d, 2H, $^2J(PtH) = 14.8$ Hz]. The ^1H NMR spectrum of the volatiles (acetone-d_6) shows Me_3SnBr: δ 0.72 [s, $^2J(SnH)_{av} = 62.9$ Hz].

Acknowledgment. We thank the NSERC of Canada for financial support.

OM970204X